Note added in proof: In a recent exchange of letters, Gregor (*13*) and Levenspiel and de Nevers (*14*) speculate on this concept. Gregor fails to account for membrane packing densities now obtainable (*10, 11*).

RICHARD S. NORMAN

Biological Sciences Group, University of Connecticut, Storrs 06268

References and Notes

1. M. King Hubbert, in *Resources and Man: A Study and Recommendations by the Committee on Resources and Man of the National Academy of Sciences–National Research Council* (Freeman, San Francisco, 1969), p. 502; *Sci. Am.* **224** (No. 3), 60 (1971); A. L. Hammond, W. D. Metz, T. H. Maugh II, *Energy and the Future* (American Association for the Advancement of Science, Washington, D.C., 1973); H. H. Landsberg and S. H. Schurr, *Energy in the United States* (Random House, New York, 1968); see also the special energy issue of *Science* (19 April 1974).
2. W. D. Metz, *Science* **180**, 1266 (1973); D. F. Othmer and O. A. Roels, *ibid.* **182**, 121 (1973); O. Levenspiel and N. de Nevers, *ibid.* **183**, 157 (1974).
3. Numerical values given here are approximate but sufficiently accurate for the purpose. In this derivation ideal solutions are assumed. See R. A. Robinson and R. H. Stokes, *Electrolyte Solutions* (Butterworth, London, rev. ed. 2, 1965), p. 242; B. F. Dodge and A. M. Eshaya, *Adv. Chem.* **27**, 7 (1960); L. A. Bromley, "Properties of Seawater and Its Concentrates and Related Solutions at Temperatures up to 400°F" [Office of Saline Water, U.S. Department of Interior Research and Development Progress Report 747 (1972)].
4. D. K. Todd, *The Water Encyclopedia* (Water Information Center, Port Washington, N.Y., 1970).
5. C. M. Summers, *Sci. Am.* **224** (No. 3), 149 (1971).
6. The power output is given by the product of the hydrostatic pressure, P, and the membrane water flux, which itself is proportional to $(P_0 - P)$. Hence power is proportional to $P(P_0 - P)$. Maximum power is obtained at $P = P_0/2$, and each cubic meter of water releases only half the theoretical energy of the reversible process.
7. A. J. Staverman, *Trans. Faraday Soc.* **48**, 176 (1952); O. Kedem and A. Katchalsky, *J. Gen. Physiol.* **45**, 143 (1961).
8. S. Sourirajan, *Reverse Osmosis* (Academic Press, New York, 1970); R. C. Riley, C. E. Milstead, H. K. Lonsdale, K. J. Mysels, "Improved Reverse Osmosis Membranes" [Office of Saline Water, U.S. Department of Interior Research and Development Progress Report 729 (1971)]; M. Clawson and H. H. Landsberg, *Desalting Seawater* (Gordon & Breach, New York, 1972).
9. An ideal system will operate at a pressure head of $P_0/2$, with seawater (concentration C_0) in the pressure chamber, and a membrane water flux of F_0, yielding power $(F_0)P_0/2$. The actual system, with concentration αC_0 in the pressure chamber, will operate at a pressure of $\alpha P_0/2$ and a membrane flux of αF_0. The pump rate, r, necessary to maintain the concentration αC_0 is $r = \alpha^2 F_0/(1-\alpha)$. The net output power is the total flow times the pressure, minus the power dissipated in the pump. Dividing by ideal power, the overall efficiency is $\alpha^2[1 + \alpha(1 - 1/E)/(1-\alpha)]$, where E is the pump efficiency. Given E, the efficiency can be maximized with respect to α, which determines the pump rate.
10. F. E. Littman, H. K. Bishop, G. Belfort, *Desalination* **11**, 17 (1972).
11. D. Stevens and S. Loeb, *ibid.* **2**, 56 (1967); K. D. B. Johnson, J. R. Grover, D. Pepper, *ibid.*, p. 40.
12. J. W. O'Meara, *ibid.* **14**, 239 (1974).
13. H. P. Gregor, *Science* **185**, 101 (1974).
14. O. Levenspiel and N. de Nevers, *ibid.*, p. 102.

3 May 1974; revised 9 July 1974

Asteroids: Surface Composition from Reflection Spectroscopy

Abstract. *Minerals partly composing the surfaces of 14 asteroids are determined by using asteroid reflectance spectra and optical properties of meteorites and other materials. Individual electronic absorption features are identified in the asteroids' spectra. The energies, relative strengths, and shapes of these features are interpreted by using laboratory and theoretical studies. Analysis of the initial 14 asteroid reflectance spectra indicates the presence of the following types of surface materials: six carbonaceous chondrite–like; two stony-iron–like (metal/silicate ~ 1); one iron meteorite–like; one basaltic achondrite–like; and four silicate-metal assemblages (metal/silicate ~ 0.25). These results support the conclusion that the asteroid belt is a source of at least some meteoritic material, and they show a relation between certain asteroids and certain classes of meteorites.*

McCord *et al.* (*1*) reported first spectral reflectance measurement of an asteroid, Vesta, with sufficient spectral resolution, range, and photometric precision to define absorption features. Between 0.3 and 1.1 μm several electronic absorption bands appeared. These features were interpreted as indicating that a magnesian pyroxene is present as the major mafic mineral and that the surface of Vesta has a composition similar to that of certain basaltic achondrite meteorites.

The first analysis of the composition of an asteroid and the direct relation uncovered between the asteroids and meteorites led to a comprehensive program of asteroid study. To date, the spectral reflectances (0.3 to 1.1 μm) of about 100 asteroids have been measured at the telescope (*2*). A comprehensive study has also been made of the optical properties of the mineral assemblages found in meteorites (*3*).

Considerable experience has been gained in using reflection spectroscopy for remote mineralogical analysis by working both with lunar sample material (*4, 5*) and with telescopic spectra for the surfaces of the moon (*6*), Mars (*7*), Mercury (*8*), and the satellites (*9*). Also, detailed laboratory studies of the optical properties of minerals and mineral assemblages have become available (*5, 10*). We have now begun to analyze the telescopic spectra for asteroids. This is a first report on the early results; a more detailed discussion will appear elsewhere (*11*).

After the success of the Vesta study (*1*), several attempts were made to determine asteroid compositions by using optical properties of meteorites. Chapman and Salisbury (*12*) compared the spectral reflectances for 36 asteroids with those for 41 meteorites. Johnson and Fanale (*13*) studied nine carbonaceous chondrite samples and one iron meteorite for comparison with asteroid spectra. These early studies utilized an empirical curve-matching technique which is less sophisticated and less generally applicable than that used in our interpretation. However, where definite interpretations were made we find good agreement between our results and those of the previous investigators.

The study reported in part here is the most extensive in terms of the variety of terrestrial, lunar, and meteoritic material used for interpretation, and great care was taken to relate optical properties to analyzed mineral constituents in the sample material. Our philosophy has been to interpret absorption features in the asteroid curves in terms of the minerals producing or modifying each feature. A set of features reveals a suite of minerals. This approach does not rely on the exact match of asteroid spectra with meteorite spectra. The meteorite sample material, which is used to study the optical properties of solids, is used as a source of mineral assemblages, the occurrence of which is cosmochemically reasonable in the asteroid belt.

The reflectance spectrum for the asteroid Ceres is shown in Fig. 1 superimposed on the reflectance spectra of 156 meteorites. The meteorite spectra are grouped according to class and therefore according to mineralogy. Note that the variation of the spectra within a class is usually less than the differences between classes. Changes in mineralogy and metamorphic grade through the classes are easily seen in the spectra.

The reflectance characteristics of the meteorite curves are understandable in terms of the type, composition, abundance, and distribution of the component mineral phases. Four spectral classes of minerals can be defined on the basis of their contribution to spectra of mixtures of phases: metals, opaques, and silicates with and without transition metal ions such as Fe^{2+} (*3*). The effect a mineral has on the spectrum is approximately proportional to its abundance and its optical density in the spectral region of interest. Opaques, cosmically most commonly represented by carbon and the carbon compounds, tend to dominate a spectrum even when present in small quantities (a few percent); an example is the carbonaceous chondrites. Opaques produce low reflectances throughout the visible and infrared spectrum and have a relatively weak ultraviolet drop-off (*13*). Silicates containing transition metal ions such as pyroxene, olivine, and feldspar) exhibit crystal field absorption features near 1 μm. The wavelength position of a band depends on the composition of the mineral (*5, 10, 11*). The symmetric, spectrally dominant 0.95-μm feature of pyroxene (as present in eucrites, howardites, and diogenites; see Fig. 1) becomes distorted by the addition of olivine (as present in ordinary chondrites). These silicate mineral assemblages are also characterized by increasingly more efficient charge transfer absorptions as one moves toward higher energies, which results in a distinct curvature of the blue and ultraviolet region of the spectral reflectance curves. Metals (Fe and Ni) become steadily more reflective toward lower energies (longer wavelengths) and the spectral reflectance of these materials exhibits a very nearly linear change with energy. The diagnostic characteristics of a spectral reflectance curve are the presence, position, and symmetry of absorption features as well as the slope and linearity and the location of inflections of the continuum.

The interpretation of two asteroid reflection spectra is treated here. The same procedure has been applied to other spectra and the results are given in Table 1.

1 Ceres. The uniform visible and infrared reflectance and the strong ultraviolet absorption indicates an opaque phase dominating the spectrum.

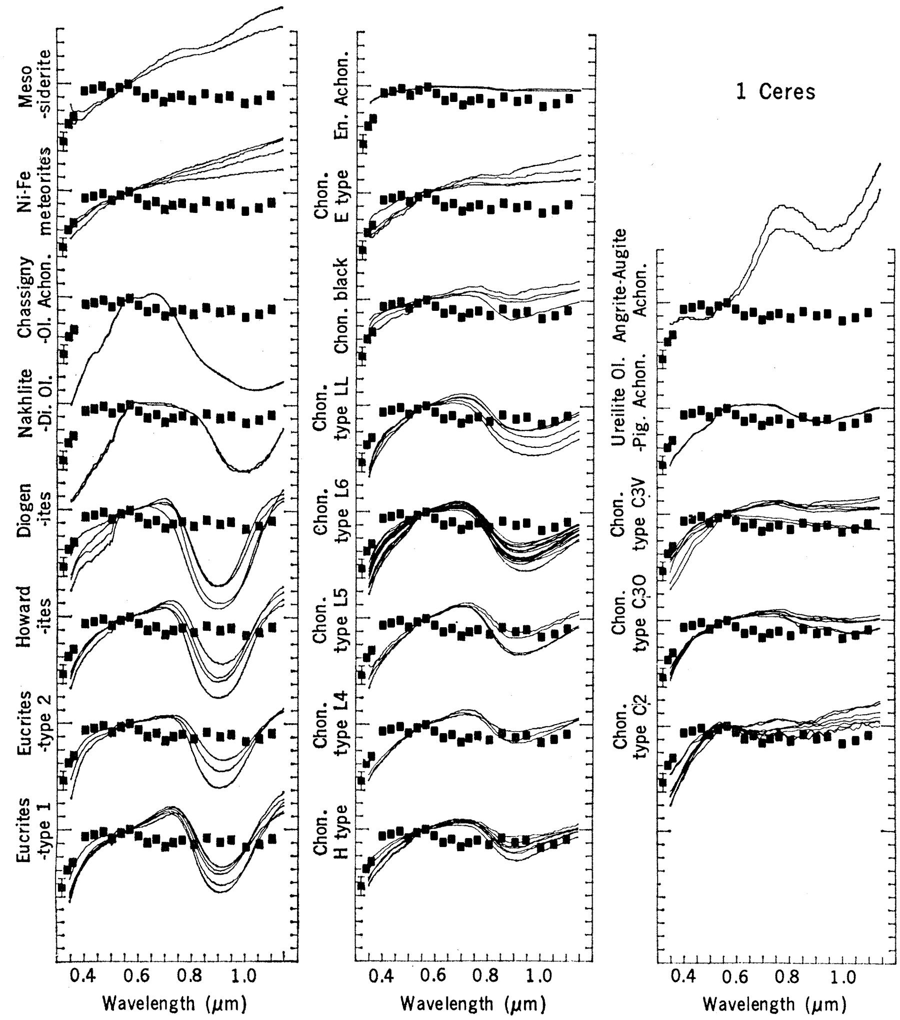

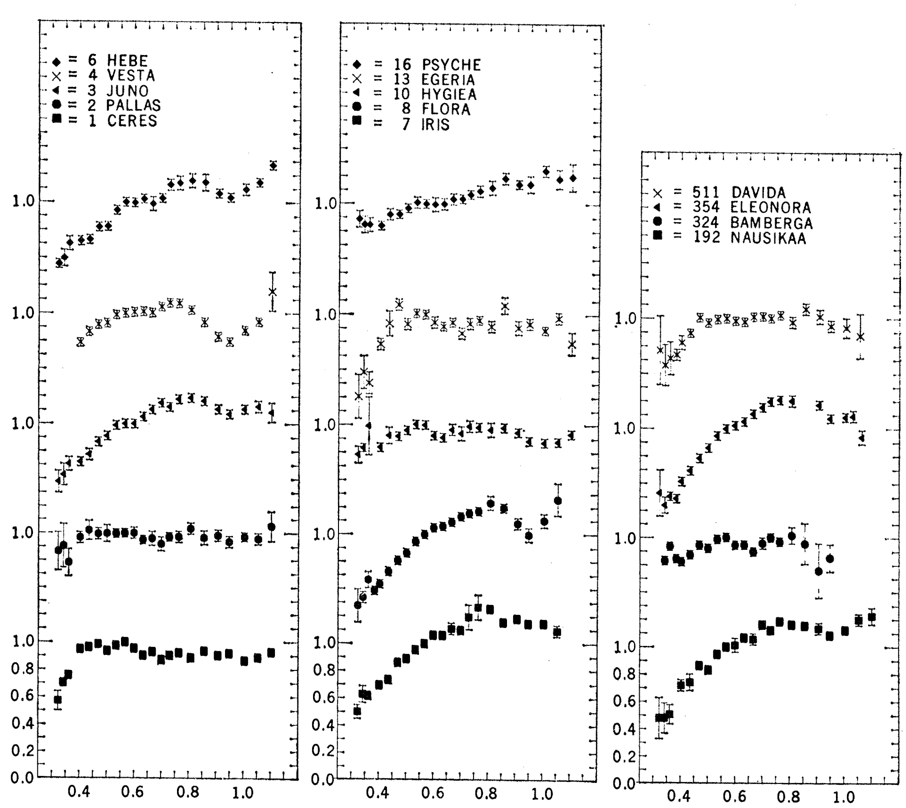

Fig. 1 (top). Spectral reflectance data for the asteroid 1 Ceres (*2*) superimposed on the spectra for 156 meteorites (*3*). The meteorite spectra are grouped according to class. Reflectance is plotted as the ordinate; each division is 0.1. All curves are scaled to unity at 0.56 μm. Abbreviations: Di., diopside; Ol., olivine; Achon., achondrite; Chon., chondrites; En., enstatite; Pig., pigeonite. Fig. 2 (bottom). Spectral reflectance data for the 14 asteroids discussed in this report. Reflectance is plotted against wavelength in micrometers. Each division in reflectance is 0.1. All points are scaled to unity at 0.56 μm.

For meteoritic material, this effect is characteristic only of the carbonaceous chondrites of higher metamorphic grade (the last three in Fig. 1). The surface of Ceres is composed of a mineral assemblage rich in opaque material (probably carbon) and probably is a type of carbonaceous chondrite material.

3 Juno. This spectrum (see Fig. 2) is characterized by a nearly linear decrease in reflectance with energy, a relatively strong, broad, asymmetric absorption near 1.0 μm, and a weak absorption near 0.6 μm. The linear reddening with decreasing energy indicates the presence of a large metal component, and the absorption features between 0.90 and 1.1 μm indicate the presence of pyroxene and olivine. Modification of the spectrum of an iron meteorite by the addition of Fe^{2+} silicate absorptions produces the best agreement with Juno's optical properties. This is an example where the direct matching technique is inappropriate and would produce spurious results.

In general, it appears that assemblages of meteoritic minerals are common in the asteroid belt (*11*). However, the distribution of petrologies found in the belt differs from that of meteorite falls. So far, carbonaceous and metal-rich silicate assemblages appear to be the most common asteroidal materials

Table 1. Some orbital parameters, diagnostic spectral features, implied minerals, and meteorite classes with similar mineral assemblages or spectral reflectance characteristics are listed for 14 asteroids. Approximate volumetric mineral proportions are given. Meteorite classes are given as indications of similar mineral assemblages and, especially with respect to the stony-iron designation, are not meant to imply a relationship to a specific meteorite. Abbreviations: *a*, semimajor axis; *e*, eccentricity; *i*, inclination; IR, infrared; UV, ultraviolet; TM, transition metal.

Asteroid	Orbital parameters	Diagnostic spectral features	Minerals most evident in spectrum	Meteorite class with similar mineral assemblage or spectral reflectivity characteristics
1 Ceres	$a = 2.77$ A.U. $e = 0.08$ $i = 10.6°$	Relatively constant visible and IR reflectance; weak UV drop-off; possi- μm; possible very weak features at 0.65 and 1.0 μm	Opaques (carbon)	Carbonaceous chondrite (intermediate metamorphic grade)
2 Pallas	$a = 2.77$ A.U. $e = 0.23$ $i = 34.8°$	Relatively constant visible and IR reflectance; weak UV drop-off; possible weak features at 0.7 and 0.95 μm	Opaques (carbon) or TM-free silicate (e.g., enstatite)	Carbonaceous chondrite (low grade) or enstatite anchondrite
3 Juno	$a = 2.67$ A.U. $e = 0.25$ $i = 13.0°$	Relatively linearly reddened visible and IR reflectance; weak feature at 0.6 μm; relatively strong, asymmetric feature at 1 μm	Metal/silicate = 1 Olivine/pyroxene = 5 Feldspar/olivine = 1	Stony-iron
4 Vesta	$a = 2.36$ A.U. $e = 0.09$ $i = 7.1°$	Nonlinearly reddened blue and visible reflectance; strong, symmetric feature at 0.95 μm; weak feature at 0.65 μm	Pyroxene Feldspar	Basaltic achondrite (eucrite)
6 Hebe	$a = 2.43$ A.U. $e = 0.21$ $i = 14.8°$	Relatively linearly reddened UV and visible reflectance; relatively strong, symmetric feature at 0.95 μm; weak feature at 0.65 μm	Metal/silicate = 1 Pyroxene	Stony-iron
7 Iris	$a = 2.39$ A.U. $e = 0.24$ $i = 5.5°$	Slightly curved UV and visible reflectance curve; decreasing reflectance > 0.8 μm (band edge)	Metal/silicate = 0.25 Feldspar/olivine = 2	
8 Flora	$a = 2.20$ A.U. $e = 0.16$ $i = 5.9°$	Very slightly curved UV and visible reflectance curve; strong, symmetric feature at 0.95 μm	Metal/silicate = 0.25 Pyroxene	
10 Hygiea	$a = 3.14$ A.U. $e = 0.10$ $i = 3.8°$	Relatively constant reflectance > 0.6 μm; relatively strong UV drop-off > 0.55 μm; relatively strong features 0.65 and 1.0 μm	Opaques (carbon) Olivine	Carbonaceous chondrite (intermediate to high grade)
13 Egeria	$a = 2.58$ A.U. $e = 0.09$ $i = 16.5°$	Relatively constant reflectance > 0.5 μm; strong UV drop-off	Opaques (carbon)	Carbonaceous chondrite (intermediate grade)
16 Psyche	$a = 2.92$ A.U. $e = 0.14$ $i = 3.1°$	Linearly reddened UV, visible, and IR reflectance	Metal	Iron meteorite
192 Nausikaa	$a = 2.40$ A.U. $e = 0.25$ $i = 6.8°$	Nonlinearly reddened UV and visible reflectance; relatively weak, symmetric feature at 0.95 μm	Pyroxene Metal (?)	
324 Bamberga	$a = 2.69$ A.U. $e = 0.36$ $i = 11.2°$	Relatively constant visible and IR reflectance; UV drop-off	Opaques (carbon)	Carbonaceous chondrite
354 Eleonora	$a = 2.80$ A.U. $e = 0.12$ $i = 18.4°$	Strong reflectance decrease > 0.8 μm; weak features at 0.65 and 0.95 μm; nearly linear UV and blue reflectance	Metal/silicate = 0.25 Olivine/pyroxene = 10 Feldspar/olivine = 2	
511 Davida	$a = 3.19$ A.U. $e = 0.17$ $i = 15.7°$	Relatively constant visible and IR reflectance; relatively strong UV drop-off; probable relatively weak feature at 1.0 μm	Opaques (carbon) Olivine (?)	Carbonaceous chondrite (intermediate grade)

observed. The mineral assemblages determined for asteroids span the range found for meteorites (rather than conforming to discrete classes). A continuous distribution of cosmologically occurring minerals may exist. A lengthy report on our interpretation of many more asteroid spectra further supporting and expanding these conclusions is in preparation (*11*).

THOMAS B. MCCORD
MICHAEL J. GAFFEY
Planetary Astronomy Laboratory, Department of Earth and Planetary Sciences, Massachusetts Institute of Technology, Cambridge 02139

References and Notes

1. T. B. McCord, J. B. Adams, T. V. Johnson, *Science* **168**, 1445 (1970).
2. C. R. Chapman, T. B. McCord, T. V. Johnson, *Astron. J.* **78**, 126 (1973); T. B. McCord and C. R. Chapman, *Astrophys. J.*, in press.
3. M. J. Gaffey, thesis, Massachusetts Institute of Technology (1974).
4. J. B. Adams and T. B. McCord, in *Proceedings of the Apollo 11 Lunar Science Conference*, A. A. Levinson, Ed. (Pergamon, New York, 1970), vol. 3, p. 19 → *Science* **171**, 567 (1971); in *Proceedings of the Second Lunar Science Conference*, A. A. Levinson, Ed. (MIT Press, Cambridge, 1971), vol. 3, p. 2138; in *Proceedings of the Fourth Lunar Science Conference*, J. W. Chamberlain and C. Watkins, Eds. (MIT Press, Cambridge, 1973), vol. 3, pp. 163–177; J. B. Adams, T. B. McCord, P. M. Bell, J. E. Conel, H. K. Mao, D. B. Nash, *Geochim. Cosmochim. Acta* **37**, 731 (1973).
5. J. B. Adams, in preparation.
6. T. B. McCord, *J. Geophys. Res.* **74**, 3131 (1968); T. V. Johnson and T. B. McCord, *Science* **169**, 885 (1970); T. B. McCord, in *The Geophysical Interpretation of the Moon*, G. Simmons, Ed. (proceedings of a conference at the Lunar Science Institute, Houston, Texas, August 1969 and June 1970), in press; ——, M. P. Charette, T. V. Johnson, L. A. Lebofsky, C. Pieters, *J. Geophys. Res.* **77**, 1349 (1972); T. V. Johnson, C. Pieters, T. B. McCord, *Icarus* **19**, 1 (1973); T. B. McCord and J. B. Adams, *Moon* **7**, 453 (1973); C. Pieters, T. B. McCord, S. H. Zisk, J. B. Adams, *J. Geophys. Res.* **78**, 5867 (1973); M. P. Charette, T. B. McCord, C. Pieters, J. B. Adams, *ibid.* **79**, 1605 (1974); C. Pieters, T. B. McCord, M. P. Charette, J. B. Adams, *Science* **183**, 1191 (1974).
7. T. B. McCord and J. A. Westphal, *Astrophys. J.* **168**, 143 (1971); ——, J. Elias, *Icarus* **14**, 245 (1971).
8. T. B. McCord, *Science* **178**, 745 (1972); —— and J. B. Adams, *Icarus* **17**, 585 (1972).
9. T. V. Johnson and T. B. McCord, *Icarus* **13**, 37 (1970); *Astrophys. J.* **169**, 589 (1971); ——, J. Elias, *ibid.* **165**, 413 (1971); C. R. Pilcher, S. T. Ridgeway, T. B. McCord, *Science* **178**, 1087 (1972).
10. J. B. Adams, *Science* **159**, 1453 (1968); in *Infrared and Raman Spectroscopy of Lunar and Terrestrial Minerals*, C. Kerr, Jr., Ed. (Academic Press, New York, in press); —— and A. L. Filice, *J. Geophys. Res.* **72**, 5705 (1967); R. G. Burns, *Mineralogical Applications of Crystal Field Theory* (Cambridge Univ. Press, Cambridge, 1970); R. L. Huguenin, *J. Geophys. Res.* **78**, 8481 (1973); *ibid.*, p. 8495; *ibid.* **79**, 3895 (1974).
11. M. J. Gaffey and T. B. McCord, in preparation.
12. C. R. Chapman and J. W. Salisbury, *Icarus* **19**, 507 (1973).
13. T. V. Johnson and F. P. Fanale, *J. Geophys. Res.* **78**, 8507 (1973).
14. This work has been supported by grants NGR 22-009-583 and NGR 22-009-473 from the National Aeronautics and Space Administration. This is MITPAL Publication No. 100.

7 June 1974; revised 29 July 1974

Volcanic Dust and Meteor Rates

Abstract. *A worldwide increase in radar meteor echo rates in 1963 correlates with the injection of massive quantities of volcanic dust into the upper atmosphere by the explosion of Mount Agung in Bali in March 1963. The consequent change in atmospheric radiative heating most probably produced the increase by changing the air density gradient.*

During the years 1960 to 1965 meteor rate surveys were conducted at the University of Canterbury, Christchurch, New Zealand (43°S, 173°E). A patrol radar with all-sky coverage was maintained in continuous operation for 3½ years during this period to gather information on the total meteor influx into the earth system. The data derived from this radar, which operated at 69.5 Mhz with a peak pulse power of 81 kw, has been reported by Ellyett and Keay (*1*) and Keay and Ellyett (*2*).

Examination of the recorded rates for 1963 showed a considerable excess in the meteor count compared to corresponding months of a previous year (*3*). Although this apparent increase amounted to some 3×10^5 echoes in 1963, it did not appreciably alter the form of the diurnal rate variation. That is, the diurnal variation for corresponding months of each year was very similar. With the year 1961 as a basis of comparison, the excess rates for 1963 were computed and are plotted in Fig. 1A.

A similar increase in radar meteor rates was also reported from Ottawa, Ontario (45°N, 76°W) (*4*), where a patrol radar was operated continuously from 1958 to 1966 at 32.7 Mhz with a peak power of 20 kw (*5*). The excess rates for the years 1963 to 1966 are plotted in Fig. 2, where the 1958–1962 rates are taken as the basis of comparison. The standard deviation shown in the pre-1963 data is also plotted on the same graph. It can be seen that the excess rates here are not as spectacular as those recorded in New Zealand, but are still well above the standard deviation values for the months of May through September.

Echoes with durations greater than 8 seconds were separated in the Canadian data, and it was shown that there was no statistically significant increase for these echoes (*4*). That is, the anomalous increase observed was restricted to the smaller meteors.

In both New Zealand and Canada the observed phenomena seem to be periodic, with an annual recurrence. The effect was first apparent in the Southern Hemisphere at the end of March 1963 and displayed a winter maximum in the months of June and July, which recurred on successive years, but with reduced magnitude. The year 1964 looks anomalously low in a series of possibly decaying peaks. In the Northern Hemisphere the effect occurred initially in May 1963, but on following years recurred in the winter months January through March or April, with 1964–1965 also being anomalously low.

The possible causal agencies of the effect are exhausted if we consider the following three spheres: extraterrestrial, man-made, or terrestrial. An extraterrestrial cause implies an increased particulate influx to the atmosphere. This influx, restricted to the smaller particles, would have had to extend over a period of some months. Although it is conceivable that planetary perturbations may have shifted the course of a single shower so that the earth now swept through its high-density core, it is difficult to imagine an agency whereby the influx was increased by the magnitude and for the duration observed. It also does not explain the fact that the recurring variations seem to be 6 months out of phase between opposite hemispheres. Furthermore, the facts that the form of the monthly mean diurnal variation remained unchanged and the ratio of maximum to minimum diurnal rates showed little scatter from year to year (*2*) seem to exclude the possibility of an increased particle influx as the cause of the rate increase.

A man-made agency suggested as a possible cause for the phenomenon was the reentry of orbiting dipoles or needles. In an experiment titled "Project West Ford," 22.7 kg of copper dipoles were dispensed into a short-lived, near polar orbit on 12 May 1963 (*6*). The objection to this explanation is that the observed increase at Christchurch commenced before the orbital injection of the dipoles, and recurred long after all trace of the dipoles had vanished (*7*). The diurnal variation of the observed rates would also be expected to show pronounced peaks every 12 sidereal hours as the observing station passed beneath the orbit.